

# Traveling Wave Profiles for a Follow-the-Leader Model for Traffic Flow with Rough Road Condition

Wen Shen\*

December 14, 2024

## Abstract

We study a Follow-the-Leader (FtL) ODE model for traffic flow with rough road condition, and analyze stationary traveling wave profiles where the solutions of the FtL model trace along, near the jump in the road condition. We derive a discontinuous delay differential equation (DDDE) for these profiles. For various cases, we obtain results on existence, uniqueness and local stability of the profiles. The results here offer an alternative approximation, possibly more realistic than the classical vanishing viscosity approach, to the conservation law with discontinuous flux for traffic flow.

**AMS Subject Classification:** 65M20, 35L65, 35L02, 34B99, 35Q99.

## 1 Introduction

We consider an ODE model for traffic flow with rough road condition. Given an index  $i \in \mathbb{Z}$  and a time  $t \geq 0$ , let  $z_i(t)$  be the position of car number  $i$  at time  $t$ . Let  $\ell$  be the length of all cars, so that

$$z_i(t) + \ell \leq z_{i+1}(t), \quad \forall t, i,$$

one defines a discrete local density  $\rho_i(t)$  for each car with index  $i$ :

$$\rho_i(t) \doteq \frac{\ell}{z_{i+1}(t) - z_i(t)}. \quad (1.1)$$

By this normalized definition, the maximum car density is  $\rho = 1$  where cars are bumper-to-bumper.

The road condition includes many factors, for example the number of lanes, quality of the road surface, surrounding situation, among other things. For simplicity of the discussion, we let  $k(x)$  be the speed limit which reflects the various road conditions. We are particularly interested in the case where  $k(x)$  is discontinuous.

---

\*Mathematics Department, Pennsylvania State University, USA. wxs27@psu.edu

At time  $t$ , given a distribution of car positions  $\{z_i(t)\}$ , the speed of each car is determined by its discrete local density and the road condition:

$$\dot{z}_i(t) = k(z_i(t)) \cdot \phi(\rho_i(t)). \quad (1.2)$$

Here  $\phi(\rho)$  is a decreasing function, with

$$\phi'(\rho) \leq -\hat{c}_0 < 0, \quad \phi(1) = 0, \quad \phi(0) = 1. \quad (1.3)$$

For example, the popular Lighthill-Whitham model [16] uses,

$$\phi(\rho) = 1 - \rho. \quad (1.4)$$

The system of ODEs (1.2) describes the *Follow-the-Leader* behavior, and is referred to as the **FtL** model. By simple computation we obtain an equivalent system of ODEs for the local densities  $\rho_i$ :

$$\dot{\rho}_i = \frac{\ell}{(z_{i+1} - z_i)^2} [\dot{z}_i - \dot{z}_{i+1}] = \frac{\rho_i^2}{\ell} [k(z_i)\phi(\rho_i) - k(z_{i+1})\phi(\rho_{i+1})]. \quad (1.5)$$

Note that given the set  $\{\rho_i\}$ , one can recover the set for the car positions  $\{z_i\}$  by  $z_{i+1} = z_i + \ell/\rho_i$ . The car position distribution  $\{z_i\}$  is unique if we fix any car, say  $z_0 = 0$ .

Let  $\{z_i(t), \rho_i(t)\}$  denote the solution of the FtL model. We seek stationary profiles  $Q(x)$  such that the points  $\{z_i(t), \rho_i(t)\}$  trace along the graph of  $Q(x)$ . To be specific, we require

$$Q(z_i(t)) = \rho_i(t) \quad \forall i, t. \quad (1.6)$$

Differentiating (1.6) in  $t$ , and using (1.2) and (1.5), we obtain

$$Q'(z_i) = \frac{\dot{\rho}_i}{\dot{z}_i} = \frac{\rho_i^2}{\ell \cdot k(z_i) \phi(\rho_i)} [k(z_i)\phi(\rho_i) - k(z_{i+1})\phi(\rho_{i+1})].$$

Using

$$z_{i+1} = z_i + \frac{\ell}{\rho_i}, \quad \rho_i = Q(z_i),$$

and writing  $x$  for  $z_i$  (since it is arbitrary), we get

$$Q'(x) = \frac{Q(x)^2}{\ell k(x) \phi(Q(x))} \cdot [k(x)\phi(Q(x)) - k(x^\sharp)\phi(Q(x^\sharp))], \quad x^\sharp = x + \frac{\ell}{Q(x)}. \quad (1.7)$$

Here  $x^\sharp$  is the location of the “leader” for the car located at  $x$ . In the literature, (1.7) belongs to a type of equations which is called a *delay differential equation* (DDE), or a *differential equation with retarded argument*.

When the road condition is uniform so that  $k(x) \equiv V$  is constant, it is known that the solutions of the FtL model converge to the scalar conservation law (cf. [7, 9, 13, 14] and references there in)

$$\rho_t + f(\rho)_x = 0, \quad f(\rho) \doteq V\rho \cdot \phi(\rho), \quad (1.8)$$

as  $\ell \rightarrow 0+$ , under suitable assumptions on the initial data. In the literature it is customary to consider the flux  $f$  a concave function with

$$f'' \leq -c_0 < 0. \quad (1.9)$$

This leads to the following reasonable assumption on  $\phi$ :

$$\phi''(\rho) < \frac{1}{\rho} [-2\phi'(\rho) + c_0/V]. \quad (1.10)$$

In this simpler case where  $k(x) = V$ , equation (1.7) takes a simpler form. Let  $W(x)$  denote this stationary profile. We have

$$W'(x) = \frac{W(x)^2}{\ell \cdot \phi(W(x))} \cdot [\phi(W(x)) - \phi(W(x^\sharp))], \quad x^\sharp = x + \frac{\ell}{W(x)}. \quad (1.11)$$

Equation (1.11) is studied by the author and collaborator in [20], where we established the existence and uniqueness of the profile  $W(x)$ , connecting two “boundary” conditions at the infinities

$$\lim_{x \rightarrow \pm\infty} W(x) = \rho_\pm, \quad \text{where } 0 \leq \rho_- \leq \rho^* \leq \rho_+ \leq 1, \quad f(\rho_-) = f(\rho_+), \quad f'(\rho^*) = 0.$$

We show that the profile  $W(x)$  is monotone and approaches  $\rho_\pm$  at an exponential rate. We also show that if  $\rho_- > \rho^*$  or  $\rho_+ < \rho^*$ , these asymptotes are unstable. Furthermore, we prove that the profile  $W(x)$  is a local attractor for nearby solutions of the FtL model.

In this paper we consider rough road condition, and analyze the behavior of solutions in the neighborhood of a discontinuity in  $k(x)$ . To fix the idea, we consider the case where  $k(x)$  is piecewise constant and has a jump at  $x = 0$ , i.e.,

$$k(x) = \begin{cases} V_+, & (x \geq 0), \\ V_-, & (x < 0). \end{cases} \quad (1.12)$$

The ODEs for  $\rho_i$  in (1.5) take the following form

$$\dot{\rho}_i = \begin{cases} \ell^{-1} V_- \rho_i^2 [\phi(\rho_i) - \phi(\rho_{i+1})], & (z_i < z_{i+1} < 0), \\ \ell^{-1} \rho_i^2 [V_- \phi(\rho_i) - V_+ \phi(\rho_{i+1})], & (z_i < 0 \leq z_{i+1}), \\ \ell^{-1} V_+ \rho_i^2 [\phi(\rho_i) - \phi(\rho_{i+1})], & (0 \leq z_i < z_{i+1}). \end{cases} \quad (1.13)$$

The system of ODEs in (1.13) has discontinuous right hand side. The discontinuity occurs twice for each  $\rho_i$ , as the car position  $z_i$  crosses  $x = 0$ , and as its leader  $z_{i+1}$  crosses  $x = 0$ .

The profile  $Q(x)$  satisfies the following *discontinuous delay differential equation* (DDDE):

$$Q'(x) = \begin{cases} \frac{Q^2}{\ell \phi(Q)} [\phi(Q) - \phi(Q(x^\sharp))], & (x^\sharp < 0 \quad \text{or} \quad x > 0), \\ \frac{Q^2}{\ell V_- \phi(Q)} [V_- \phi(Q) - V_+ \phi(Q(x^\sharp))], & (x < 0 < x^\sharp), \end{cases} \quad (1.14)$$

where  $x^\sharp = x + \ell/Q(x)$  is the position for the leader of the car at  $x$ . Note that for the first case in (1.14) the equation is the same as (1.11). For the second case, behind the jump in  $k(x)$ , it is different,

Formally, as  $\ell \rightarrow 0$ , the car density function  $\rho$  satisfies the following conservation law:

$$\rho_t + f(k(x), \rho)_x = 0, \quad \text{where } f(k(x), \rho) \doteq k(x)\rho\phi(\rho). \quad (1.15)$$

Here  $k(x)$  is discontinuous at  $x = 0$ . Two types of jumps occur in the solution, the  $k$ -jump at  $x = 0$  and the  $\rho$ -shock where  $k$  is constant. The  $\rho$ -shock and its corresponding traveling wave profiles of the FtL model is studied in [20], where existence, uniqueness and local stability are proved. In this paper we consider the  $k$ -jump at  $x = 0$ , and analyze the stationary profile  $Q(x)$  that connects the two constant states  $\rho_\pm$  as  $x \rightarrow \pm\infty$ .

There are various cases, with different relations between  $(V_-, V_+)$  and  $(\rho_-, \rho_+)$ . For each of these cases, we study the initial value problem for (1.14), with initial data given on  $x \geq 0$ . Due to the discontinuity in the coefficient  $k(x)$ , the analysis is non-trivial. We establish the key condition of transversality of the vector field with respect to the curves of discontinuity, which in term yields the existence and well-posedness of the solutions for the initial value problem. For literature on discontinuous ODEs and transversality condition, we refer to [4–6, 10] and the references therein.

We also show that the solution of the initial value problem with suitable initial data gives the desired stationary profile  $Q(x)$ . For different cases we prove that: (i) there exist infinitely many profiles, (ii) there exists exactly one profile, or (iii) no profile exists. Depending on the case, some of the profiles attract nearby solutions for the FtL model, while others are unstable.

We compare our result to the classical vanishing viscosity approach. The conservation law (1.15) can be approximated by a viscous equation

$$\rho_t + f(k(x), \rho)_x = \varepsilon \rho_{xx}, \quad (1.16)$$

where  $\varepsilon > 0$  is a small parameter representing the viscosity. When  $k(x)$  has a jump as in (1.12), the  $k$ -jump at  $x = 0$  has a corresponding stationary viscous profile  $\rho^\varepsilon(x)$ , satisfying the ODE

$$\frac{d}{dx} \rho^\varepsilon(x) = \frac{1}{\varepsilon} [f(k(x), \rho^\varepsilon(x)) - \bar{f}], \quad \bar{f} = f(V_-, \rho_-) = f(V_+, \rho_+). \quad (1.17)$$

Monotone viscous profiles exist if one of the following hold:

- We have  $\rho_- < \rho_+$  and there exists a  $\hat{\rho} \in [\rho_-, \rho_+]$  such that

$$f(V_-, \rho) > \bar{f} \text{ for } \rho \in [\rho_-, \hat{\rho}], \quad \text{and} \quad f(V_+, \rho) > \bar{f} \text{ for } \rho \in [\hat{\rho}, \rho_+].$$

- We have  $\rho_- > \rho_+$  and there exists a  $\hat{\rho} \in [\rho_+, \rho_-]$  such that

$$f(V_-, \rho) < \bar{f} \text{ for } \rho \in [\rho_+, \hat{\rho}], \quad \text{and} \quad f(V_+, \rho) < \bar{f} \text{ for } \rho \in [\hat{\rho}, \rho_-].$$

See [11, 12, 18]. For other general references on scalar conservation law with discontinuous coefficient, we refer to a survey paper [1] and the references therein. On related references on micro-macro models for traffic flow and their analysis, we refer to [2, 3, 8, 17].

The rest of the paper is organized as follows. In section 2 we present various technical Lemmas, on specific properties for the solutions of (1.14) and (1.11). Section 3 is dedicated to the case with  $V_- > V_+$ , where 4 sub-cases are analyzed in detail. The analytical result is also confirmed by numerical simulations. The case with  $V_- < V_+$  is studied in section 4, following a similar line of approach as in section 3. The analysis for the main sub case here is much more involving due to the lack of monotonicity. Finally, concluding remarks are given in section 5.

## 2 Technique Lemmas

For the rest of the paper, we denote the flux functions

$$f_-(\rho) \doteq V_- \rho \phi(\rho), \quad f_+(\rho) \doteq V_+ \rho \phi(\rho). \quad (2.1)$$

Since the jump is stationary, the Rankine-Hugoniot condition requires

$$f_-(\rho_-) = f_+(\rho_+) \doteq \bar{f} \geq 0. \quad (2.2)$$

We note that the cases with  $\bar{f} = 0$  are trivial, since they represent the cases where the road is either empty or completely bumper-to-bumper. Indeed, if  $\rho_- = \rho_+ = 0$  then there is no car on the road; if  $\rho_- = \rho_+ = 1$  then the road is completely bumper-to-bumper with cars; and if  $\rho_- = 0, \rho_+ = 1$ , then there is no car on  $x < 0$  but completely bumper-to-bumper on  $x > 0$ . For the rest of the discussion, we assume

$$\bar{f} > 0, \quad \text{i.e. } 0 < \rho < 1.$$

We start with some definitions.

**Definition 2.1.** Let  $Q(x)$  be a continuous function defined on  $x \in \mathbb{R}$  with  $0 < Q(x) < 1$ . We call a sequence of car positions  $\{z_i\}$  a **distribution of car positions generated by  $Q(x)$** , if

$$\rho_i = Q(z_i), \quad z_{i+1} - z_i = \frac{\ell}{Q(z_i)}, \quad \forall i \in \mathbb{Z}. \quad (2.3)$$

Here  $\rho_i$  is the discrete density for the  $i$ th car. If one imposes  $z_0 = 0$ , then the distribution  $\{z_i\}$  is unique.

**Definition 2.2.** Given a profile  $Q(x)$  and a distribution of car positions  $\{z_i(t)\}$ . Let  $\{\rho_i(t)\}$  be the corresponding discrete densities for the cars, computed as (1.1). We say that  $\{z_i(t)\}$  **traces along  $Q(x)$** , if

$$Q(z_i(t)) = \rho_i(t), \quad \forall i \in \mathbb{Z}, t \geq 0.$$

The following Lemma is immediate.

**Lemma 2.1.** *Let  $Q(x)$  be a given profile and  $\{z_i(0)\}$  be a distribution generated by  $Q(x)$ . Let  $\{z_i(t)\}$  be the solution of (1.2) with initial data  $\{z_i(0)\}$ . Then,  $Q(x)$  satisfies (1.7) if and only if  $\{z_i(t)\}$  traces along  $Q(x)$ .*

Solutions of (1.7) exhibit periodical behaviors.

**Lemma 2.2. (Periodicity.)** *Let a continuous function  $Q(x)$  be given on  $x \in \mathbb{R}$  with  $0 < Q(x) < 1$ , and let  $\{z_i(t)\}$  be a distribution of car positions generated by  $Q(x)$ . Then the followings are equivalent.*

- (a)  $Q(x)$  satisfies the equation (1.7);
- (b) There exist a constant period  $t_p$  such that

$$z_i(t + t_p) = z_{i+1}(t), \quad \forall i \in \mathbb{Z}, t \geq 0. \quad (2.4)$$

*Proof.* We first prove that (b) implies (a). Indeed, since the system is autonomous, we can set  $t = 0$ . Writing

$$z_i(0) = x, \quad z_{i+1}(0) = x^\sharp = x + \ell/Q(x),$$

and using

$$\frac{dz}{dt} = k(z) \cdot \phi(Q(z)), \quad \rightarrow \quad \frac{dz}{k(z) \cdot \phi(Q(z))} = dt,$$

the time it takes for car no  $i$  to reach the position of its leader is

$$t_p = \int_x^{x+\ell/Q(x)} \frac{1}{k(z)\phi(Q(z))} dz = \text{constant}.$$

Differentiating the above equation in  $x$  on both sides, one gets

$$(1 - \ell Q'(x)/Q^2(x)) \frac{1}{k(x^\sharp)\phi(Q(x^\sharp))} - \frac{1}{k(x)\phi(Q(x))} = 0,$$

which easily leads to (1.7). The proof for (a) implies (b) can be obtained by reversing the order of the above arguments.  $\square$

The next lemma is also immediate.

**Lemma 2.3.** *In the setting of Lemma 2.2, if we have*

$$\lim_{x \rightarrow \infty} Q(x) = \rho_+, \quad \lim_{x \rightarrow -\infty} Q(x) = \rho_-, \quad f_-(\rho_-) = f_+(\rho_+) = \bar{f}, \quad (2.5)$$

*then the period is determined as*

$$t_p = \frac{\ell}{\bar{f}}. \quad (2.6)$$

*On the other hand, if the period  $t_p$  is given and the solution approach some asymptotic limits as  $x \rightarrow \pm\infty$ , then they must be  $\rho_\pm$  with*

$$f_-(\rho_-) = f_+(\rho_+) = \frac{\ell}{t_p}.$$

Next Lemma shows that the solution  $Q(x)$  is monotone in some kind of “average”.

**Lemma 2.4.** *Let  $Q(x)$  be a profile that satisfies (1.7). Given  $x$ , we let*

$$x^\sharp = x + \ell/Q(x)$$

*be the position of the leader for the car at  $x$ . Then, for any  $x$ , we have*

$$\frac{\ell}{\bar{f}} - \frac{\ell}{f(k(x), Q(x))} = \int_x^{x^\sharp} \left[ \frac{1}{k(z)\phi(Q(z))} - \frac{1}{k(x)\phi(Q(x))} \right] dz. \quad (2.7)$$

*When  $k(x) \equiv V$  is constant on  $[x, x^\sharp]$ , (2.7) simplifies to*

$$\frac{\ell}{\bar{f}} - \frac{\ell}{f(V, Q(x))} = \frac{1}{V} \int_x^{x^\sharp} \left[ \frac{1}{\phi(Q(z))} - \frac{1}{\phi(Q(x))} \right] dz. \quad (2.8)$$

*Proof.* The Lemma follows immediately from the periodicity property in Lemma 2.2

$$\frac{\ell}{\bar{f}} = \int_x^{x^\sharp} \frac{1}{k(z)\phi(Q(z))} dz.$$

Since  $\phi' < 0$ , the mapping  $\rho \mapsto (1/\phi(\rho))$  is monotone increasing. Then, (2.8) roughly says that if  $f(V, Q(x)) > \bar{f}$  at some  $x$ , then some “averaged-value” of  $Q$  on  $[x, x^\sharp]$  is larger than  $Q(x)$ , so in “average”  $Q(x)$  is increasing. Similarly, if  $f(V, Q(x)) < \bar{f}$  at some  $x$ , then in “average”  $Q(x)$  is decreasing.  $\square$

We now establish the invariant regions  $Q(x) > \rho_-$  and  $Q(x) > \rho_+$ , for  $x < 0$ .

**Lemma 2.5.** *Let  $k(x)$  be the step function in (1.12), and let  $Q(x)$  be a profile that satisfies (1.14) with*

$$\lim_{x \rightarrow \infty} Q(x) = \rho_+, \quad \bar{f} = f_+(\rho_+).$$

*Let  $I = [y, y^\sharp]$  be the interval where*

$$y^\sharp = y + \ell/Q(y) \leq 0.$$

*Then, the followings hold.*

- (a) *If  $f_-(Q(x)) > \bar{f}$  for  $x \in I$ , then  $f_-(Q(x)) > \bar{f}$  for all  $x \leq y$ .*
- (b) *If  $f_-(Q(x)) < \bar{f}$  for  $x \in I$ , then  $f_-(Q(x)) < \bar{f}$  for all  $x \leq y$ .*

*In both cases, we have*

$$\lim_{x \rightarrow -\infty} Q(x) = \rho_- \quad \text{where } \rho_- < \rho^* \text{ and } f_-(\rho_-) = \bar{f}.$$

*Proof.* We prove (a) by contradiction, while the proof for (b) is completely similar. Suppose that  $f_-(Q(x)) > \bar{f}$  for  $x \in I$ . Then  $Q(x) > \rho_-$  on  $I$ . Now assume the opposite, such that  $Q(x)$  can be less than  $\rho_-$  for  $x \leq y$ . Let  $\bar{y}$  be the right most point where  $Q(x)$  crosses  $\rho_-$ , such that

$$Q(\bar{y}) = \rho_-, \quad Q(x) > \rho_- \quad \text{for } x > \bar{y}. \quad (2.9)$$

Now (2.8) implies that the “average” value of  $Q(x)$  on the interval  $[\bar{y}, \bar{y} + \ell/Q(\bar{y})]$  is  $\rho_-$ . Clearly, this contradicts (2.9).

To prove the asymptotic limit, let  $\{z_i\}$  be a distribution of car position generated by  $Q(x)$  with  $z_0 = y^\sharp$ , and denote the interval  $I_k = [z_k, z_{k+1}]$ . Let

$$M_k \doteq \max_{x \in I_k} \frac{1}{\phi(Q(x))}, \quad k < 0,$$

and let  $\{y_k\}$  be the points where these maxima are attained:

$$\frac{1}{\phi(Q(y_k))} = M_k.$$

We claim that

$$M_{k+1} - M_k \geq \mathcal{O}(1) \cdot (Q(z_k) - \rho_-), \quad \text{for } k < -2, \quad (2.10)$$

which implies that

$$\lim_{k \rightarrow -\infty} M_k = 1/\rho_-, \quad \text{so} \quad \lim_{x \rightarrow -\infty} Q(x) = \rho_-.$$

Indeed, if  $Q(x)$  is monotone on  $I_{-2}$ , then it must be monotone increasing due to (2.8). An induction argument shows that  $Q(x)$  is monotone on  $x \leq z_{-2}$ . Then  $M_k = Q(z_{k+1})$ , and (2.8) implies

$$M_k - M_{k-1} \geq Q(z_k) \left( \frac{1}{\rho_- \phi(\rho_-)} - \frac{1}{Q(z_k) \phi(Q(z_k))} \right) \geq \mathcal{O}(1) \cdot (Q(z_k) - \rho_-).$$

If  $Q(x)$  is not monotone, then  $M_k$  is attained at a local maximum, say  $y_k \in I_k$ . Denote its leader as  $y_k^\sharp$  where  $y_k^\sharp \in I_{k+1}$  and  $Q(y_k) = Q(y_k^\sharp)$ . Then (2.8) implies that there exists a local maximum  $y'_{k+1} \in (y_k, y_k^\sharp)$ , and

$$Q(y'_{k+1}) - Q(y_k) \geq Q(y_k) \left( \frac{1}{\rho_- \phi(\rho_-)} - \frac{1}{Q(y_k) \phi(Q(y_k))} \right) \geq \mathcal{O}(1) \cdot (Q(y_k) - \rho_-).$$

Since

$$M_{k+1} - M_k \geq Q(y'_{k+1}) - Q(y_k),$$

we complete the proof.  $\square$

**Lemma 2.6. (Ordering of the profiles.)** *Assume that there exists multiple profiles that solves the equation (1.14) with asymptotes  $\rho_\pm$  that satisfies (2.2). Then the graphs of these profiles never intersect.*

*Proof.* We prove by contradiction. Assume that there exist two profiles  $Q_1(x), Q_2(x)$  which intersect at a point  $y$ , such that

$$Q_1(y) = Q_2(y), \quad Q_1(x) > Q_2(x) \text{ for } x > y.$$

Let  $y^\sharp \doteq y + \frac{\ell}{Q(y)}$  be the position of the leader for the car at  $y$ , and let  $t_{p,1}, t_{p,2}$  be the times for the car at  $y$  to reach its leader's position at  $y^\sharp$ , tracing along  $Q_1(x), Q_2(x)$ , respectively. Then

$$t_{p,1} = \int_y^{y^\sharp} \frac{1}{k(x)\phi(Q_1(x))} dx > \int_y^{y^\sharp} \frac{1}{k(x)\phi(Q_2(x))} dx = t_{p,2}.$$

Since both profiles  $Q_1, Q_2$  approach the same asymptotic limits, by Lemma 2.3 one must have  $t_{p,1} = t_{p,2}$ , a contraction.  $\square$

### 3 Case 1: $V_- > V_+$ .

In this section we consider the case where the speed limit has a downward jump at  $x = 0$ . Recall the Rankine-Hugoniot jump condition (2.2). Fix a  $\bar{f}$ , with

$$0 < \bar{f} \leq f_+(\rho^*), \quad \text{where } f'_-(\rho^*) = f'_+(\rho^*) = 0,$$

and let  $\rho_{1,2}^\pm$  be the unique values that satisfy

$$f_\pm(\rho_{1,2}^\pm) = \bar{f}, \quad 0 < \rho_1^- < \rho_1^+ \leq \rho^* \leq \rho_2^+ < \rho_2^- < 1. \quad (3.1)$$

Note that we may have  $\rho_1^+ = \rho^* = \rho_2^+$  when  $\bar{f} = f_+(\rho^*)$ . See Figure 1 for an illustration.

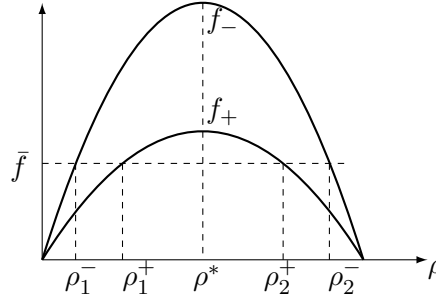


Figure 1: Flux functions  $f_-$ ,  $f_+$ , and location of  $\rho_{1,2}^\pm$ , which are candidates for  $\rho_\pm$ .

There are 4 possible combinations of  $(\rho_-, \rho_+)$  which satisfy (2.2):

- 1A.  $(\rho_-, \rho_+) = (\rho_1^-, \rho_2^+)$ , i.e.,  $0 < \rho_- < \rho^* < \rho_+ < 1$ ;
- 1B.  $(\rho_-, \rho_+) = (\rho_1^-, \rho_1^+)$ , i.e.,  $0 < \rho_- < \rho_+ \leq \rho^*$ ;
- 1C.  $(\rho_-, \rho_+) = (\rho_2^-, \rho_2^+)$ , i.e.,  $\rho^* < \rho_+ < \rho_- < 1$ ;

1D.  $(\rho_-, \rho_+) = (\rho_2^-, \rho_1^+)$ , i.e.,  $0 < \rho_+ \leq \rho^* < \rho_- < 1$ .

We denote by  $W(x)$  the unique stationary profile that satisfies (1.11), with

$$W(0) = \rho^*, \quad \lim_{x \rightarrow -\infty} W(x) = \rho_1^+, \quad \lim_{x \rightarrow +\infty} W(x) = \rho_2^+. \quad (3.2)$$

Note that any horizontal shifts of  $W(x)$  is again a solution of (1.11). The existence and uniqueness of such a profile is proved in [20].

We discuss each subcase in detail in the rest of this section.

### 3.1 Case 1A: $0 < \rho_- < \rho^* < \rho_+ < 1$ .

**Existence of solutions.** Since  $\rho_+$  is a stable asymptote, on  $x > 0$  the solution for  $Q(x)$  must be either some horizontal shift of  $W(x)$  or the trivial solution  $Q(x) = \rho_+$ . For different horizontal shifts, these profiles take different values of  $Q(0)$ . In all cases, we have

$$\rho_1^+ < Q(0) \leq \rho_+.$$

Once  $Q(x)$  is given for  $x \geq 0$ , one can solve (1.14) backward in  $x$  as an “initial value problem”. It is understood that the derivative in (1.14) is the left derivative, as one solves the equations backward in  $x$ . The profile  $Q(x)$ , if exists, can have kinks, but remains continuous. Next Theorem provides well-posedness of this initial value problem.

**Theorem 3.1. (Well-posedness of Initial Value Problem)** *Let  $V_- > V_+$ . Given  $\rho_+$  such that  $\rho^* < \rho_+ < 1$ . Let  $Q(x)$  be the solution of (1.14) on  $x < 0$ , with initial data given on  $x \geq 0$  as either a horizontal shift of  $W(x)$  or the constant function  $\rho_+$ . Then there exists a unique monotone solution of  $Q(x)$  on  $x < 0$ .*

*Proof.* The proof takes a couple of steps.

**Step 1.** In the  $(x, Q)$  plane, let  $\mathcal{C}_0$  be the vertical line where  $x = 0$ , and let  $\mathcal{C}_1$  be the graph of the function  $h(x) = -\ell/x$ . The curve  $\mathcal{C}_1$  indicates the position and local density of the cars whose leader is at  $x = 0$ . The discontinuities in (1.14) occurs along  $\mathcal{C}_0$  and  $\mathcal{C}_1$ . To ensure the existence and uniqueness of solutions, the vector field of the DDDE (1.14) must be **transversal** to the curves of discontinuity.

Along  $\mathcal{C}_0$ , the discontinuity line is vertical, with infinite tangent. Thus, we need  $Q'(0\pm)$  to be bounded. This is easily verified from (1.14), since  $Q(0) \leq \rho_+ < 1$  so  $\phi(Q(0)) > 0$ .

Along the curve  $\mathcal{C}_1$ , the tangent at a point  $(x, h(x))$  is

$$h'(x) = \ell/x^2 = h(x)^2/\ell.$$

Let  $Q(x)$  be a profile that solves (1.14), and let  $y < 0$  be its intersection point with  $\mathcal{C}_1$  such that  $Q(y) = h(y)$ . We claim that

$$Q'(y\pm) < h'(y). \quad (3.3)$$

Indeed, from (1.14) we have

$$\begin{aligned} Q'(y-) &= \frac{h(y)^2}{\ell \cdot \phi(h(y))} [\phi(h(y)) - \phi(Q(0))] = h'(y) \left[ 1 - \frac{\phi(Q(0))}{\phi(h(y))} \right], \\ Q'(y+) &= \frac{h(y)^2}{\ell V_- \phi(h(y))} [V_- \phi(h(y)) - V_+ \phi(Q(0))] = h'(y) \left[ 1 - \frac{V_- \phi(Q(0))}{V_+ \phi(h(y))} \right]. \end{aligned}$$

Thus (3.3) holds since  $Q(0) < 1$  and  $\phi(Q(0)) > 0$ .

**Step 2.** Once the transversality property is established, the existence and uniqueness of the solution for  $Q(x)$  is achieved by iteration. Denote  $I_k = [-k\ell, -k\ell + \ell]$ , for  $k = 1, 2, 3, \dots$ . Consider  $I_1$ . If  $x \in I_1$ , then its leader  $x^\sharp$  is located at

$$x^\sharp = x + \ell/Q(x) > 0.$$

We have an ODE with discontinuous right hand side, with

$$Q'(x) = \frac{Q(x)^2}{\ell \cdot V_- \phi(Q(x))} [V_- \phi(Q(x)) - V_+ \phi(Q(x^\sharp))] \quad (3.4)$$

where  $Q(x^\sharp)$  is given by the initial data on  $x \geq 0$ . Standard theory for discontinuous ODEs (see [4]) gives an uniqueness solution on  $I_1$ , provided that  $Q(x)$  satisfies  $0 < Q(x) < 1$  on  $I_1$ . Indeed, the lower bound of 0 is obvious. To prove the upper bound, we claim that  $Q'(x) > 0$  on  $I_1$ . We argue with contradiction. Assuming that  $Q(x)$  is not monotone on  $I_1$ , then there exists a point  $y \in I_1$  such that

$$Q'(y) = 0, \quad Q'(x) \geq 0 \quad \text{for } x > y.$$

Since  $Q'(0-) > 0$ , then  $y < 0$ , and we have

$$Q(y) < Q(y^\sharp), \quad y^\sharp = y + \ell/Q(y) > 0. \quad (3.5)$$

Now (3.4) and  $Q'(y) = 0$  imply

$$V_- \phi(Q(y)) - V_+ \phi(Q(y^\sharp)) = 0.$$

Since  $V_- > V_+$  and  $\phi' < 0$ , we get

$$Q(y) > Q(y^\sharp),$$

a contradiction to (3.5).

**Step 3.** We iterate the argument in Step 2 for  $k = 2, 3, \dots$ , until  $I_k$  crosses the curve  $C_1$ . After that, (3.4) is replaced by

$$Q'(x) = \frac{Q(x)^2}{\ell \cdot \phi(Q(x))} [\phi(Q(x)) - \phi(Q(x^\sharp))], \quad x^\sharp = x + \ell/Q(x) < 0. \quad (3.6)$$

The the argument follows, proving existence and uniqueness of a monotone solution  $Q(x)$  on  $x < 0$ , for the initial value problem.  $\square$

Next Corollary establishes the existence of many monotone profiles  $Q(x)$  that connects  $\rho_-$  and  $\rho_+$ .

**Corollary 3.1.** *Let*

$$V_- > V_-, \quad 0 < \rho_- \leq \rho^* \leq \rho_+ < 1, \quad f_-(\rho_-) = f_+(\rho_+).$$

*There exist infinitely many monotone profiles  $Q(x)$  which satisfy (1.14) and*

$$\rho_1^+ < Q(0) \leq \rho_+, \quad (3.7)$$

*and the boundary conditions*

$$\lim_{x \rightarrow -\infty} Q(x) = \rho_-, \quad \lim_{x \rightarrow +\infty} Q(x) = \rho_+. \quad (3.8)$$

*Moreover, these profiles never intersect with each other.*

*Proof.* In Theorem 3.1 we show that there exist many profiles  $Q(x)$  that satisfy (1.14), (3.7), and the second boundary condition in (3.8). Let  $Q(x)$  be such a profile. It remains to show that the first boundary condition in (3.8) holds. Since  $Q(x)$  is monotone and bounded below by 0, then there exists an asymptotic limit as  $x \rightarrow -\infty$ . By Lemma 2.3 this limit must be  $\rho_-$ .

The non-intersecting property of the profiles follows from Lemma 2.6.  $\square$

Sample profiles are illustrated in Figure 2 plot (2), using

$$V_- = 2, \quad V_+ = 1, \quad \ell = 0.2, \quad \phi(\rho) = 1 - \rho, \quad \bar{f} = 3/16.$$

**Viscous Profiles.** As comparison, we illustrate the stationary viscous profiles. For this case there exist infinitely many stationary monotone viscous profiles that satisfy the ODE (1.17). For each value of  $\rho^\varepsilon(0) \in (\rho_1^+, \rho_+]$ , there exists a unique viscous profile. Sample viscous profiles with  $\varepsilon = 0.2$  are given in Figure 2 plot (3).

**Local Stability of the Profiles.** We have shown that for each given  $Q(0)$  on the interval  $(\rho_1^+, \rho_+]$ , there exists a unique profile. Let  $Q^\sharp(x)$  be the profile with  $Q^\sharp(0) = \rho_+$ , and let  $Q^\flat(x)$  be the limit profile as  $Q(0) \rightarrow \rho_1^+$ . We define the domain

$$D \doteq \left\{ (x, y) : Q^\flat(x) < y \leq Q^\sharp(x), x \in \mathbb{R} \right\}. \quad (3.9)$$

Clearly all profiles of  $Q(x)$  lie in  $D$ . We now show that  $D$  is a basin of attraction of the solution of the FtL, in the sense described below.

Since all the profiles in  $D$  never cross each other, we can parametrize the family of profiles, say by the value  $Q(0)$ . By continuity, any point  $(x, y) \in D$  belong to a unique profile, call it  $Q_{(x,y)}$  such that

$$Q_{(x,y)}(x) = y.$$

For any point  $(x, y) \in D$ , we define the function

$$\Psi(x, y) \doteq Q_{(x,y)}(0), \quad (x, y) \in D. \quad (3.10)$$

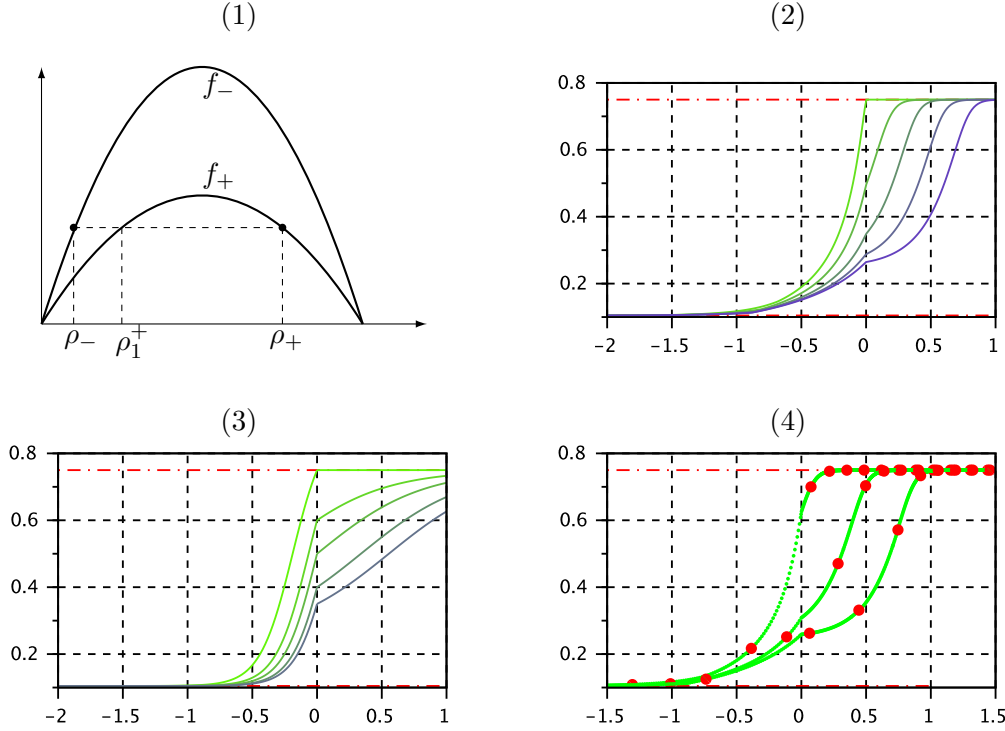


Figure 2: Case 1A: (1) Flux functions; (2) Plots of  $Q(x)$ ; (3) Plots of  $\rho^\varepsilon(x)$ ; (4) Solutions of the FtL model.

**Theorem 3.2.** Consider the setting of Corollary 3.1 and let  $D$  be defined as in (3.9). Let  $\{z_i(0)\}$  be a set of initial car positions and  $\{\rho_i(0)\}$  be the corresponding discrete density defined as (1.1), and assume that

$$(z_i(0), \rho_i(0)) \in D, \quad \forall i \in \mathbb{Z}. \quad (3.11)$$

Let  $\{z_i(t)\}$  be the solution of the FtL model with this initial data, and let  $\{\rho_i(t)\}$  be its discrete density. Then

$$(z_i(t), \rho_i(t)) \in D, \quad \forall t > 0, \quad \forall i \in \mathbb{Z}. \quad (3.12)$$

Let

$$\Psi_i(t) = \Psi(z_i(t), \rho_i(t)), \quad i \in \mathbb{Z},$$

and define the total variation

$$TV\{\Psi_i(t)\} \doteq \sum_i |\Psi_i(t) - \Psi_{i+1}(t)|.$$

Then, we have

$$\lim_{t \rightarrow \infty} TV\{\Psi_i(t)\} = 0, \quad \text{i.e.,} \quad \lim_{t \rightarrow \infty} \Psi_i(t) = \tilde{\Psi}, \quad \forall i \in \mathbb{Z}. \quad (3.13)$$

Thus, asymptotically the points  $\{z_i(t), \rho_i(t)\}$  trace along the profile  $Q(x)$  with  $Q(0) = \tilde{\Psi}$ .

*Proof.* It suffices to show the followings:

- (i) If  $\Psi_m(\tau) > \Psi_{m+1}(\tau)$  at time  $\tau$  for some  $m$ , then  $\frac{d}{dt}\Psi_m(\tau) < 0$ ; and
- (ii) If  $\Psi_n(\tau) < \Psi_{n+1}(\tau)$  at time  $\tau$  for some  $n$ , then  $\frac{d}{dt}\Psi_n(\tau) > 0$ .

We prove (i) while (ii) can be proved in an entirely similar way. Let  $\hat{Q}(x)$  be the profile that passes through the point  $\{z_m(\tau), \rho_m(\tau)\}$ . By the assumption  $\Psi_m(\tau) > \Psi_{m+1}(\tau)$ , and the point  $\{z_{m+1}(\tau), \rho_{m+1}(\tau)\}$  lies below the profile  $\hat{Q}(x)$ , i.e.,

$$\hat{Q}(z_{m+1}(\tau)) > \rho_{m+1}(\tau). \quad (3.14)$$

It then suffices to show that

$$\frac{\dot{\rho}_m(\tau)}{\dot{z}_m(\tau)} < \hat{Q}'(z_m(\tau)), \quad (3.15)$$

indicating that the point  $(z_m(\tau), \rho_m(\tau))$  moves below the profile  $\hat{Q}(x)$  as  $t$  increases from  $\tau$ . Indeed, equation (1.7) gives

$$\hat{Q}'(z_m) = \frac{\hat{Q}^2(z_m)}{\ell k(z_m)\phi(\hat{Q}(z_m))} \left[ k(z_m)\phi(\hat{Q}(z_m)) - k(z_{m+1})\phi(\hat{Q}(z_{m+1})) \right]. \quad (3.16)$$

On the other hand, (1.2) and (1.5) give

$$\frac{\dot{\rho}_m(\tau)}{\dot{z}_m(\tau)} = \frac{\rho_m^2}{\ell k(z_m)\phi(\rho_m)} [k(z_m)\phi(\rho_m) - k(z_{m+1})\phi(\rho_{m+1})]. \quad (3.17)$$

Since  $\rho_m = \hat{Q}(z_m)$ , together with (3.14), we conclude (3.15).  $\square$

Numerical approximations are computed for the solutions of the FtL model with the following ‘‘Riemann initial data’’,

$$z_i(0) = \begin{cases} i\ell/\rho_+, & i \geq x_0, \\ i\ell/\rho_-, & i < x_0, \end{cases} \quad \rho_i(0) = \begin{cases} \rho_+, & i \geq x_0, \\ \rho_-, & i < x_0. \end{cases} \quad (3.18)$$

The simulations are carried out for  $0 \leq t \leq 2$ , and we plot the trajectory of  $z_i(t)$  in green for the last period

$$2 - \ell/\bar{f} \leq t \leq 2,$$

together with the car positions at  $t = 2$  as red dots, in Figure 2 plot (4). The 3 profiles in the plot are for

$$x_0 = 0, \quad x_0 = 0.3\ell/\rho_-, \quad \text{and} \quad x_0 = 0.6\ell/\rho_-.$$

Even though the initial data points  $\{z_i(0), \rho_i(0)\}$  are not entirely in  $D$ , nevertheless we observe that the solutions of FtL model converge quickly to certain profiles of  $Q(x)$ , suggesting that Theorem 3.2 probably applies to a bigger neighborhood.

### 3.2 Case 1B: $0 < \rho_- < \rho_+ \leq \rho^*$ .

Since  $\rho^+$  is an unstable asymptote for  $x \rightarrow +\infty$ , the only solution on  $x \geq 0$  is the constant solution  $Q(x) \equiv \rho_+$ . Once  $Q(x)$  is given on  $x > 0$ , the rest can be solved backward in  $x$  using (1.14), as an initial value problem. The existence and uniqueness of the profile follows the same argument as for Theorem 3.1 and Corollary 3.1. We summarize the result in next Theorem.

**Theorem 3.3.** *Let  $V_- > V_+$  and  $0 < \rho_- < \rho_+ \leq \rho^*$  with  $f_-(\rho_-) = f_+(\rho_+)$ . There exists a unique monotone profile  $Q(x)$  which satisfies the equation (1.14) with*

$$Q(x) = \rho_+ \quad \text{for } x \geq 0, \quad \lim_{x \rightarrow -\infty} Q(x) = \rho_-.$$

A typical plot of  $Q(x)$  is given in Figure 3 plot (2), where the dashed red line is the value of  $\rho_-$ . As comparison, we also plot the viscous profile  $\rho^\varepsilon(x)$  in Figure 3 plot (3), with  $\rho^\varepsilon(x) = \rho_+$  on  $x \geq 0$ . This is the only viscous profile that connects the two limit values  $\rho_\pm$  at  $x \rightarrow \pm\infty$ .

**Instability.** Since  $\rho_+$  is an unstable asymptote, the profile is unstable with respect to perturbations on  $x > 0$ , and the solution of the FtL model can not converge to the profile in the sense of Theorem 3.2. Even if one starts with “Riemann” initial data with  $\rho_i(0) = \rho_+$  for all  $z_i(0) \geq 0$ , the perturbation, initially on  $x < 0$ , will propagate into the region  $x > 0$ . Numerical simulation verifies this fact, see Figure 3 plot (4), where a perturbation is formed and moves into  $x > 0$ . Although on  $x < 0$  the FtL solution gets very close to the profile  $Q$ , the stability can not be achieved on  $x > 0$ . This forward propagating wave is caused by the fact that the characteristic speed satisfies

$$f'_-(\rho_-) > 0, \quad f'_+(\rho_-) > 0,$$

therefore information travels to the right.

### 3.3 Case 1C: $\rho^* < \rho_+ < \rho_- < 1$ .

Since  $\rho_-$  is an unstable asymptote as  $x \rightarrow -\infty$ , one must have

$$Q(x) \equiv \rho_- \quad \text{for } x < 0.$$

Now consider the value  $Q(0+)$ . Since  $Q'(-\ell/\rho_-) = 0$ , equation (1.14) implies

$$V_- \phi(Q(-\ell/\rho_-)) = V_+ \phi(Q(0+)) \quad \rightarrow \quad Q(0+) < Q(-\ell/\rho_-) = Q(0-).$$

This implies that  $Q(x)$  is discontinuous at  $x = 0$ , which is not possible for the solution of (1.14). We have the following Theorem.

**Theorem 3.4.** *Let  $V_- > V_+$  and  $\rho^* < \rho_+ < \rho_- < 1$  with  $f_-(\rho_-) = f_+(\rho_+)$ . There exists no profile  $Q(x)$  that satisfies (1.14) and the boundary conditions (3.8).*

We remark that there exists a unique viscous profile for this case, see Figure 4 plot (2). We also plot the solution of the FtL model with this “Riemann data”, see Figure 4 plot (3). Observe that the solution is highly oscillatory on  $x < 0$ , and it never settles, indicating no convergence as  $t$  grows.

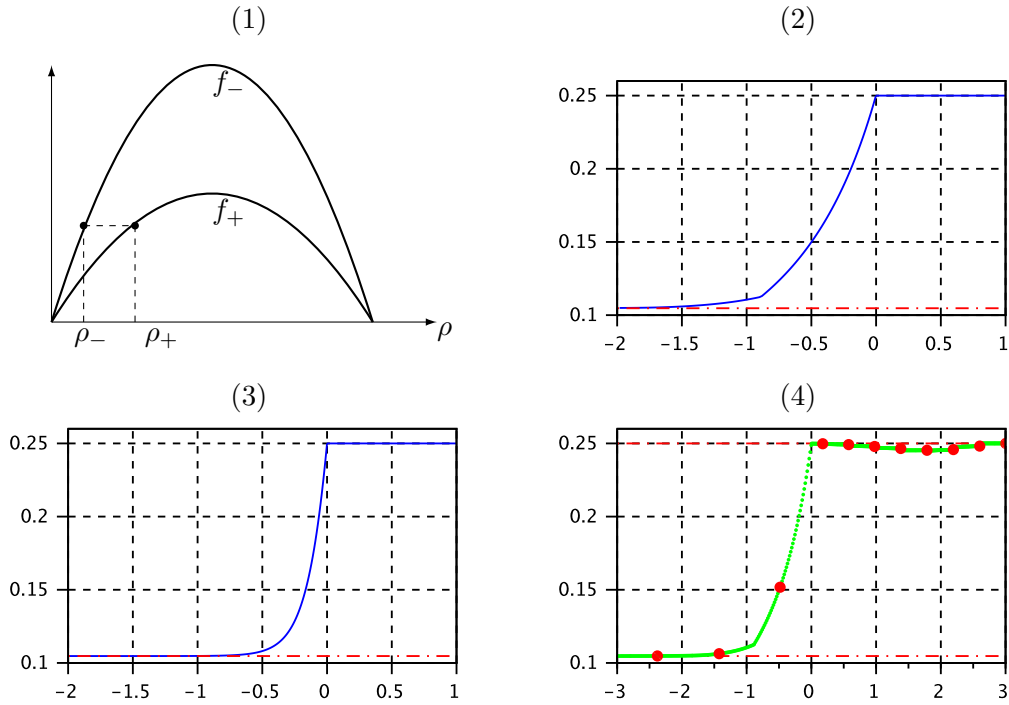


Figure 3: Case 1B. Plots for  $Q(x)$ ,  $\rho^\varepsilon(x)$ , and solutions of the FtL model.

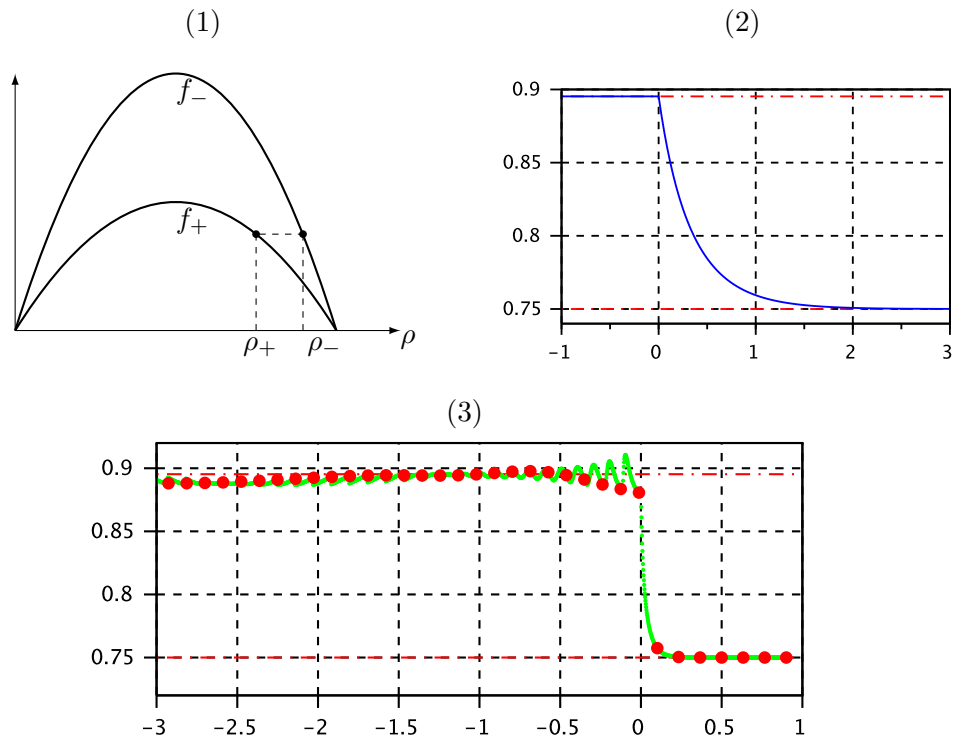


Figure 4: Case 1C. (2): Viscous profile  $\rho^\varepsilon(x)$ ; (3): solution of the FtL model.

### 3.4 Case 1D: $0 < \rho_+ \leq \rho^* < \rho_- < 1$ .

Since both  $\rho_{\pm}$  are unstable asymptotes, one must have  $Q(x) = \rho_-$  on  $x < 0$  and  $Q(x) = \rho_+$  on  $x > 0$ , which is not possible.

**Theorem 3.5.** *Let  $V_- > V_+$  and  $0 < \rho^* < \rho_- < 1$  with  $f_-(\rho_-) = f_+(\rho_+)$ . There exists no profile  $Q(x)$  that satisfies (1.14) and the boundary conditions (3.8).*

There are no monotone viscous profiles either. In Figure 5 we plot numerical simulation result for the FtL model, with “Riemann data”. We observe oscillatory behavior on  $x < 0$ , and a rarefaction wave behavior on  $x > 0$ . The solution does not settle into any profile as  $t$  grows.

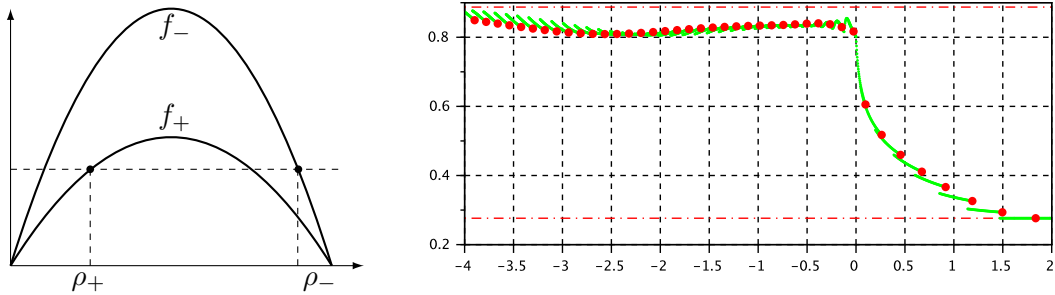


Figure 5: Case 1D. Solution for the FtL model.

### 4 Case 2: $V_- < V_+$ .

In this section we study the case where the speed limit has an upward jump at  $x = 0$ . The discussion for this case follows a similar path as for Case 1, but with rather different details. Given  $\bar{f}$ , which is in the range of both  $f_{\pm}$ , the candidates for  $\rho_{\pm}$  are illustrated in Figure 6, with

$$0 < \rho_1^+ < \rho_1^- \leq \rho^* \leq \rho_2^- < \rho_2^+.$$

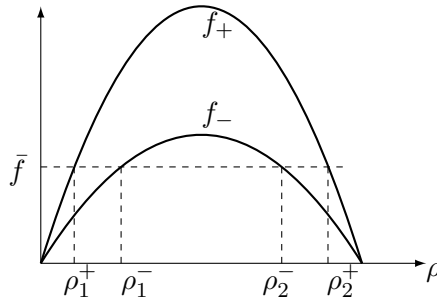


Figure 6: Flux functions  $f_-$ ,  $f_+$ , and location of  $\rho_{1,2}^{\pm}$ , which are candidates for  $\rho_{\pm}$ .

We have the following 4 sub-cases:

- Case 2A:  $\rho_- = \rho_1^-$  and  $\rho_+ = \rho_2^+$ , such that  $0 < \rho_- \leq \rho^* \leq \rho_+ < 1$ ;
- Case 2B:  $\rho_- = \rho_1^-$  and  $\rho_+ = \rho_1^+$ , such that  $0 < \rho_+ < \rho_- < \rho^*$ ;
- Case 2C:  $\rho_- = \rho_2^-$  and  $\rho_+ = \rho_2^+$ , such that  $\rho^* < \rho_- < \rho_+ < 1$ ;
- Case 2D:  $\rho_- = \rho_2^-$  and  $\rho_+ = \rho_1^+$ , such that  $0 < \rho_+ < \rho^* < \rho_- < 1$ .

#### 4.1 Case 2A: $0 < \rho_- \leq \rho^* \leq \rho_+ < 1$ .

Here both  $\rho_-$  and  $\rho_+$  are stable asymptotic limits as  $x \rightarrow -\infty$  and  $x \rightarrow +\infty$ , respectively. Then, on  $x > 0$ , the profile  $Q(x)$  must be some horizontal shift of  $W(x)$ . Using this as “initial condition”, one can solve (1.7) backward in  $x$ . In next Theorem we establish unique solutions of the initial value problems for (1.14), which give us the profiles  $Q(x)$  that satisfy the proper boundary conditions at the limit  $x \rightarrow \pm\infty$ .

**Theorem 4.1.** *Let  $V_- < V_+$ . Given  $\rho_+$  such that  $\rho^* < \rho_+ < 1$ . Let  $Q(x)$  be the solution of (1.14) on  $x < 0$ , with initial data given on  $x \geq 0$  as some horizontal shift of  $W(x)$  where  $Q(0)$  satisfies*

$$\rho_1^+ \leq Q(0) \leq \rho_2^-. \quad (4.1)$$

*Then there exists a unique solution  $Q(x)$  on  $x < 0$  for this initial value problem. Furthermore,*

$$\lim_{x \rightarrow -\infty} Q(x) = \rho_-, \quad \rho_- < \rho^*, \quad f_-(\rho_-) = f_+(\rho_+), \quad (4.2)$$

*such that each of these solutions is a solution to (1.14) with boundary conditions*

$$\lim_{x \rightarrow \pm\infty} Q(x) = \rho_{\pm}. \quad (4.3)$$

*Proof.* This Theorem is the counter part of Theorem 3.1 and Corollary 3.1 for Case 1A, but the proof here is much more involving due to the lack of monotonicity. See Figure 7.

Let the initial data be given on  $x \geq 0$  as some horizontal shift of  $W(x)$  such that (4.1) holds. Denote by  $Q(x)$  the solution for this initial value problem, solved backward in  $x$ . Then  $Q(x)$  is monotone on  $x \geq 0$  with  $Q'(x) > 0$ . Let  $\{z_i\}$  be a car position distribution generated by  $Q(x)$  with  $z_0 = 0$  and

$$z_k + \frac{\ell}{Q(z_k)} = z_{k+1}, \quad \forall k \in \mathbb{Z}.$$

We also denote the intervals

$$I_k \doteq (z_k, z_{k+1}), \quad \text{for } k \in \mathbb{Z}.$$

Throughout the rest of the proof, we use the simplified notations, for any index  $k$ ,

$$Q_k = Q(z_k), \quad \phi_k = \phi(Q(z_k)). \quad (4.4)$$

The proof takes several steps.

**Step 1.** Assume that  $Q(x)$  is a solution of the initial value problem, with the additional condition

$$\rho_- \leq Q_0 \leq \rho_2^- . \quad (4.5)$$

We claim that

$$Q'(0-) > 0. \quad (4.6)$$

Indeed, since  $Q'(x) > 0$  for  $x > 0$ , by (2.8) we have

$$\frac{1}{\phi_1} - \frac{1}{\phi_0} > Q_0 V_+ \left[ \frac{1}{\bar{f}} - \frac{1}{f_+(Q_0)} \right]. \quad (4.7)$$

By using  $\bar{f} \leq V_- Q_0 \phi_0$  and (4.7), we get

$$\begin{aligned} \frac{1}{V_+ \phi_1} - \frac{1}{V_- \phi_0} &= \frac{1}{V_+} \left[ \frac{1}{\phi_1} - \frac{1}{\phi_0} \right] + \frac{1}{V_+ \phi_0} - \frac{1}{V_- \phi_0} \\ &> Q_0 \left[ \frac{1}{\bar{f}} - \frac{1}{f_+(Q_0)} \right] + \frac{1}{V_+ \phi_0} - \frac{1}{V_- \phi_0} \geq 0. \end{aligned} \quad (4.8)$$

Equation (1.14) leads to

$$Q'(0-) = \frac{Q_0^2}{\ell V_+ \phi_1} \left[ \frac{1}{V_+ \phi_1} - \frac{1}{V_- \phi_0} \right] > 0.$$

**Step 2.** We claim that on the interval  $I_{-1}$  there doesn't exist any local maximum. Indeed, assume local maxima exist, and let  $y_1$  be the right most local maximum, with  $Q'(y_1) = 0$ . Let  $y_1^\sharp > 0$  be its leader. By (1.14) and  $Q'(y_1) = 0$ , we get

$$V_- \phi(Q(y_1)) = V_+ \phi(Q(y_1^\sharp)). \quad (4.9)$$

Moreover, there exists a point  $y_2$ , such that

$$y_1 < y_2 < 0, \quad Q(y_2) < Q(y_1), \quad Q'(y_2) < 0.$$

Let  $y_2^\sharp > 0$  be its leader, where  $y_2^\sharp > y_1^\sharp > 0$ . Since  $Q'(x) > 0$  on  $x > 0$ , we must have

$$Q(y_2^\sharp) > Q(y_1^\sharp), \quad \Rightarrow \quad \phi(Q(y_2^\sharp)) < \phi(Q(y_1^\sharp)). \quad (4.10)$$

By (1.14) and  $Q'(y_2) < 0$ , we get

$$V_+ \phi(Q(y_2^\sharp)) > V_- \phi_2 > V_- \phi_1 = V_+ \phi(Q(y_1^\sharp)),$$

a contradiction to (4.10).

**Step 3.** We now show that, if (4.5) holds, then

$$Q_{-1} < Q_0. \quad (4.11)$$

Indeed, we know that there are no local maxima on  $I_{-1}$  and  $Q'(0-) > 0$ . If  $Q(x)$  is monotone increasing on  $I_{-1}$ , the result trivially holds. Now consider the case where  $Q(x)$  has a local minimum. We assume the opposite, such that there exist a point  $y \in (z_{-1}, 0)$  where

$$Q(y) = Q(0) = Q_0, \quad Q(x) < Q_0 \quad \text{for } x \in (y, 0).$$

Let  $y^\sharp$  be its leader, where  $0 < y^\sharp < z_1$ . Recall (2.7), we have

$$\begin{aligned} \int_y^{y^\sharp} \left[ \frac{1}{k(z)\phi(Q(z))} - \frac{1}{V_-\phi(Q(y))} \right] dz &= \int_y^{y^\sharp} \left[ \frac{1}{k(z)\phi(Q(z))} - \frac{1}{V_-\phi_0} \right] dz \\ &= \frac{\ell}{\bar{f}} - \frac{\ell}{f_-(Q(y))} = \frac{\ell}{\bar{f}} - \frac{\ell}{f_-(Q_0)} \doteq \gamma \geq 0, \end{aligned}$$

which gives

$$\gamma = \int_y^0 \left[ \frac{1}{V_-\phi(Q(z))} - \frac{1}{V_-\phi_0} \right] dz + \int_0^{y^\sharp} \left[ \frac{1}{V_+\phi(Q(z))} - \frac{1}{V_-\phi_0} \right] dz.$$

Since the first integrand on the right hand side is strictly negative, we get

$$\int_0^{y^\sharp} \left[ \frac{1}{V_+\phi(Q(z))} - \frac{1}{V_-\phi_0} \right] dz > \gamma. \quad (4.12)$$

But (4.12) is not possible. Indeed, since  $Q'(x) > 0$  on  $x > 0$ , the mapping  $x \mapsto (1/\phi(Q(x)))$  is increasing. Using that

$$\frac{1}{V_+\phi(Q_0)} - \frac{1}{V_-\phi(Q_0)} < 0, \quad \int_0^{z_1} \left[ \frac{1}{V_+\phi(Q(z))} - \frac{1}{V_-\phi(Q_0)} \right] dz = \gamma,$$

one reaches

$$\int_0^x \left[ \frac{1}{V_+\phi(Q(z))} - \frac{1}{V_-\phi(Q_0)} \right] dz < \gamma, \quad \text{for any } x \in (0, z_1),$$

a contradiction to (4.12).

**Step 4.** Assume now  $Q(x)$  is a profile that satisfies

$$0 < Q(z_{-1}) < \rho_-. \quad (4.13)$$

We claim that

$$\lim_{x \rightarrow -\infty} Q(x) = \rho_-. \quad (4.14)$$

Indeed, if on  $I_{-2}$   $Q(x)$  stays on one side of  $\rho_-$ , then Lemma 2.5 provides the results. If  $Q(x)$  crosses  $\rho_-$ , we apply a similar argument as the proof for Lemma 2.5. Let

$$M_k = \max \left\{ \max_{x \in I_k} \frac{1}{\phi(Q(x))}, \frac{1}{\phi(\rho_-)} \right\}.$$

Assume that for  $M_k > 1/\phi(\rho_-)$  for some  $k$ , and let  $y_k \in I_k$  be the point where  $M_k = \phi(Q(y_k))^{-1}$ , and let  $y_k^\sharp \in I_{k+1}$  denote the position of its leader. Then  $Q(y_k) = Q(y_k^\sharp)$ , and (2.8) implies

$$M_{k+1} - M_k \geq Q(y_k) \left[ \frac{1}{\rho_- \phi(\rho_-)} - \frac{1}{Q(y_k) \phi(Q(y_k))} \right] \geq \mathcal{O}(1) \cdot \left[ \frac{1}{\phi(Q(y_k))} - \frac{1}{\phi(\rho_-)} \right].$$

Thus, we conclude that

$$\lim_{k \rightarrow -\infty} M_k = \frac{1}{\phi(\rho_-)}.$$

Therefore on  $x \leq 0$  there exists an upper envelope  $E^\flat(x)$  for  $Q(x)$ , such that

$$Q(x) \leq E^\sharp(x), \quad \lim_{x \rightarrow -\infty} E^\sharp(x) = \rho_-. \quad (4.15)$$

A symmetrical argument for the local minima below  $\rho_-$  leads to a lower envelope  $E^\flat(x)$  on  $x < 0$  for  $Q(x)$ , with

$$E^\flat(x) < \rho_-, \quad \lim_{x \rightarrow -\infty} E^\flat(x) = \rho_-. \quad (4.16)$$

The result (4.14) follows from a squeezing argument.

**Step 5.** Denote by  $Q^\sharp(x)$  the profile with  $Q^\sharp(0) = \rho_2^-$ . By Step 3, we have

$$0 < Q^\sharp(z_{-1}) < Q^\sharp(0) = \rho_2^-.$$

By Step 4, such a profile exists and satisfies (4.14). By the transversality property, the solution is unique.

Then, any profile  $Q(x)$  with  $\rho_1^+ < Q(0) < \rho_2^-$  lies below  $Q^\sharp(x)$ , and thus

$$0 < Q(z_{-1}) < \rho_2^-.$$

Therefore, a unique profile exists and satisfies (4.14), completing the proof.  $\square$

Sample profiles of  $Q(x)$  are plotted in Figure 7 plot (2), where we observe that the profiles are not monotone. We also plot multiple viscous profiles  $\rho^\varepsilon(x)$  in Figure 7 plot (3), as a comparison. Note that if  $\rho^\varepsilon(0) \in (\rho_-, \rho_+)$ , the viscous profiles are monotone, a property not preserved by  $Q(x)$ .

**Local Stability of the Profiles.** As in the setting of Theorem 3.2, let  $Q^\sharp(x)$  be the profile with  $Q^\sharp(0) = \rho_2^-$ , and let  $Q^\flat(x)$  be the limit profile as  $Q(0) \rightarrow \rho_1^+$ . Similar to Case 1A, we define a basin of attraction as (3.9). All profiles lie in  $D$ , where they do not intersect with each other. Parametrizing the region with these profiles, as in Theorem 3.2, we get the same local stability property. We skip the details.

Again, numerical simulations are performed for the FtL model, as for Case 1A, and we plot the solutions with ‘‘Riemann data’’ (3.18). See Figure 7 plot (4). We see the clear convergence to a certain profile for each choice of initial data.

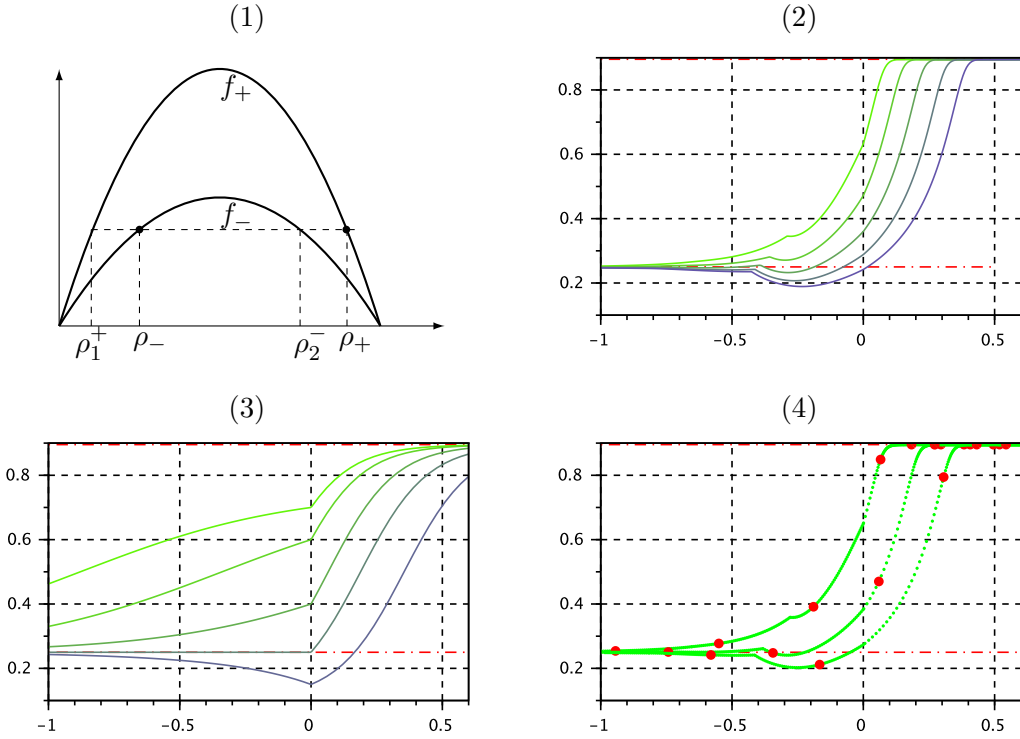


Figure 7: Case 2A.

#### 4.2 Case 2B: $0 < \rho_+ < \rho_- < \rho^*$ .

This is similar to Case 1B. Since  $\rho_+$  is an unstable asymptote for  $x \rightarrow \infty$ , we must have  $Q(x) \equiv \rho_+$  on  $x \geq 0$ . Using this as the initial data, one can solve  $Q(x)$  backward in  $x$ . Since  $\rho_-$  is a stable asymptote, we have  $Q(x) \rightarrow \rho_-$  as  $x \rightarrow -\infty$ . Thus there exists a unique monotone profile  $Q(x)$ . For the same reason as for case 1B, this profile is not a local attractor for the solutions of the FtL model.

In Figure 8 we plot the profile  $Q(x)$  in plot (2), the viscous profile  $\rho^\varepsilon(x)$  in plot (3), and the solution of the FtL model with ‘‘Riemann data’’ in plot (4). Note that a perturbation enters the region  $x > 0$ , even with initial Riemann data, indicating the instability of the profile  $Q(x)$ .

#### 4.3 Case 2C: $\rho^* < \rho_- < \rho_+ < 1$ .

This is the corresponding case as for Case 1C. With the same argument, one concludes that there doesn’t exist any profile  $Q(x)$ , although a viscous profile  $\rho^\varepsilon(x)$  does exist. See Figure 9 plot (2). The solution of the FtL model plot (3) demonstrates severe oscillation on  $x < 0$  which never settles in time.

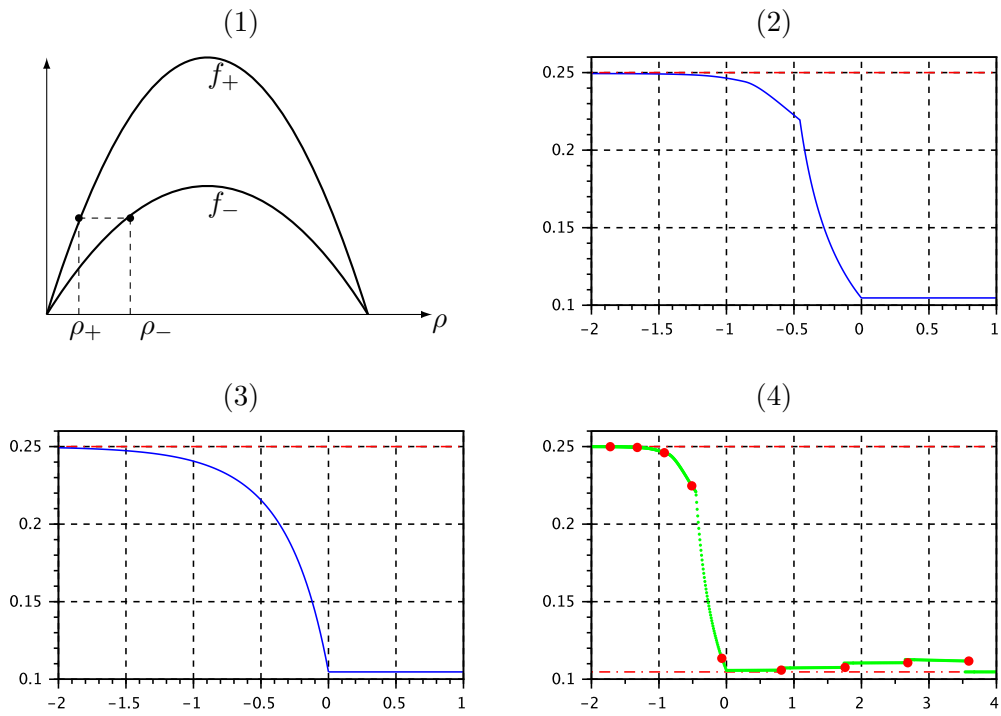


Figure 8: Case 2B.

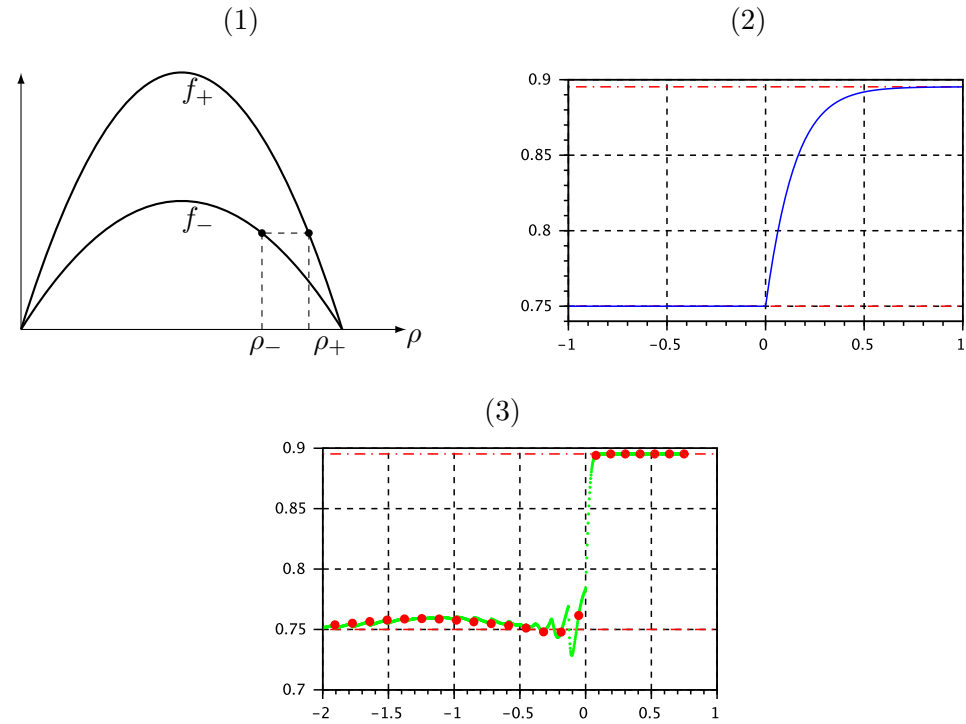


Figure 9: Case 2C. Plot of the viscous profile  $\rho^\epsilon$  and a solution for the FtL model.

#### 4.4 Case 2D: $0 < \rho_+ < \rho^* < \rho_- < 1$ .

For this case, we have neither the profile  $Q(x)$  nor the viscous profile  $\rho^\varepsilon(x)$ . We plot some solution of the FtL model in Figure 10, which doesn't converge to any profile as time grows.

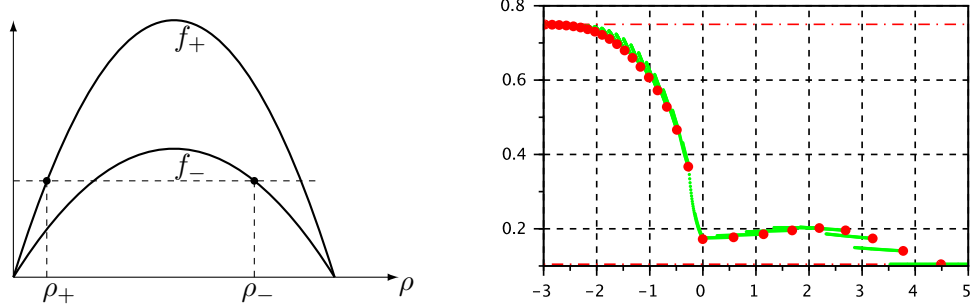


Figure 10: Case 2D. Solution of the FtL model.

#### 4.5 A Numerical Simulation

We perform numerical simulation to obtain approximate solution for the FtL model, with “Riemann” initial data  $(\rho^L, \rho^R)$  such that

$$\rho_i(0) = \begin{cases} \rho^R, & i \geq 0, \\ \rho^L, & i < 0, \end{cases} \quad z_i(0) = \begin{cases} i\ell/\rho^R, & i \geq 0, \\ i\ell/\rho^L, & i < 0, \end{cases} \quad z_0(0) = 0.$$

We choose values of  $(\rho^L, \rho^R)$  such that

$$f_-(\rho^L) \neq f_+(\rho^R).$$

We use

$$\phi(\rho) = 1 - \rho, \quad (V_-, V_+) = (2, 1), \quad \rho^L = 0.6, \quad \rho^R = 0.7, \quad \ell = 0.01.$$

See results in Figure 11, at time  $t = 1$ . The flux functions  $f_-, f_+$  and the locations of  $\rho^{L,R}$  are illustrated in plot (1), while the solution  $\{z_i(T), \rho_i(T)\}$  of the FtL model is in plot (2). As a comparison, we also simulate the viscous conservation law

$$\rho_t + f(k(x), \rho)_x = \varepsilon \rho_{xx},$$

using the same Riemann data, with  $\varepsilon = 0.02$  and  $k(x)$  the jump function (1.12). The result is in plot (3).

The vanishing viscosity limit solution for the conservation law (1.15) consists of a shock with negative speed from L to M, and a stationary jump from M to R. The solution of the FtL model captures this main feature. However, due to the instability of the path M-R where the left state is unstable, we observe oscillations behind the stationary jump at  $x = 0$ . We remark that the solution of the viscous conservation law with the same initial data does not contain oscillation behind  $x = 0$ .

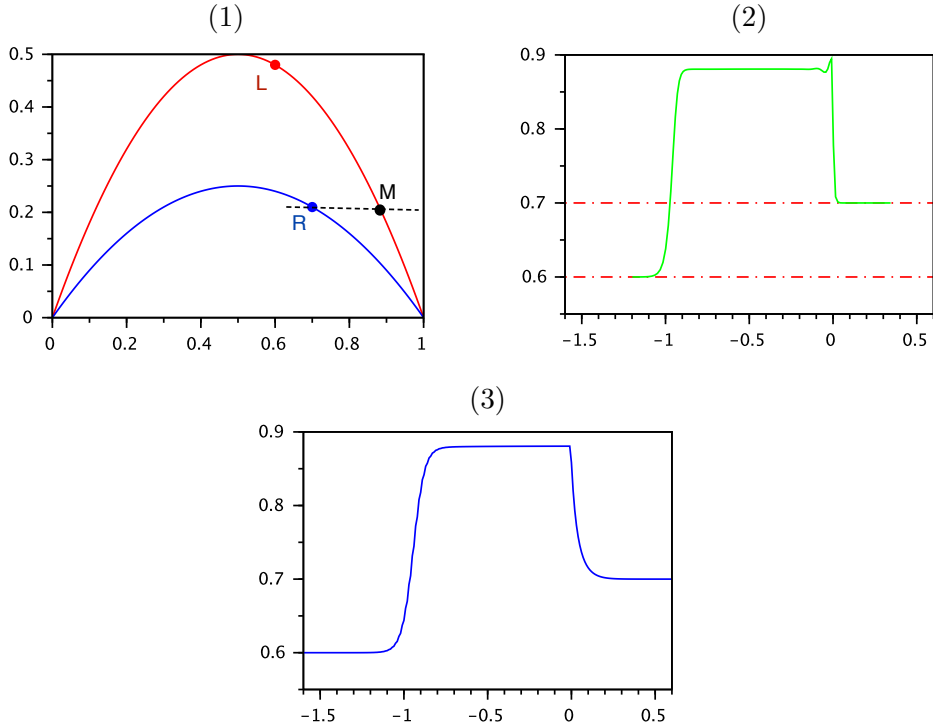


Figure 11: Numerical simulation results with FtL model and the viscous conservation law, with Riemann initial data.

## 5 Concluding Remarks

In this paper we derive a discontinuous delay differential equation for the stationary traveling wave profile for an ODE model of traffic flow, where the road condition is discontinuous. For various cases, we obtain results on the existence, uniqueness and local stability of the profiles.

These results offer alternative approximate solutions to the scalar conservation law with discontinuous flux, as a counter part to the classical vanishing viscosity approach. The stabilizing effect of the viscosity is not entirely present in the FtL model, where oscillations are observed behind the discontinuity in the road condition. This is caused by the “directional” influence in real life traffic, where the drivers adjust their behavior only according to situations ahead of them, not what is behind. Heuristically, this fact contributes to the “lack of viscosity” behind the jump at  $x = 0$ , and thus the oscillations.

The natural followup work is to investigate the converge of solutions of the FtL model, under suitable assumptions, to some entropy admissible solution of the scalar conservation law with discontinuous flux. We expect this to be a challenging task, due to the non-monotone profiles and oscillations behind the jump in the road condition.

One may criticize the FtL model of being too simple, especially around the jump in the road condition, where the drivers change their speed suddenly as they cross  $x = 0$ . The

model is a first order approximation where one assumes instant acceleration. A high order model, where the acceleration is finite, might smooth out the behavior near  $x = 0$  and remove the oscillations. However, such model would take the velocities of the cars as unknowns, and thus become much more complex.

## References

- [1] B. Andreianov, *New approaches to describing admissibility of solutions of scalar conservation laws with discontinuous flux*, CANUM 2014—42e Congrès National d’Analyse Numérique, ESAIM Proc. Surveys, vol. 50, EDP Sci., Les Ulis, 2015, pp. 40–65, DOI 10.1051/proc/201550003. MR3416038
- [2] J.-P. Aubin, *Macroscopic traffic models: shifting from densities to “celerities”*, Appl. Math. Comput. **217** (2010), no. 3, 963–971, DOI 10.1016/j.amc.2010.02.032. MR2727134
- [3] N. Bellomo, A. Bellouquid, J. Nieto, and J. Soler, *On the multiscale modeling of vehicular traffic: from kinetic to hydrodynamics*, Discrete Contin. Dyn. Syst. Ser. B **19** (2014), no. 7, 1869–1888, DOI 10.3934/dcdsb.2014.19.1869. MR3253235
- [4] A. Bressan, *Unique solutions for a class of discontinuous differential equations*, Proc. Amer. Math. Soc. **104** (1988), no. 3, 772–778, DOI 10.2307/2046790. MR964856
- [5] A. Bressan and W. Shen, *Uniqueness for discontinuous ODE and conservation laws*, Nonlinear Anal. **34** (1998), no. 5, 637–652, DOI 10.1016/S0362-546X(97)00590-7. MR1634652
- [6] ———, *Unique solutions of discontinuous O.D.E.’s in Banach spaces*, Anal. Appl. (Singap.) **4** (2006), no. 3, 247–262, DOI 10.1142/S0219530506000772. MR2239406
- [7] R. M. Colombo and E. Rossi, *On the micro-macro limit in traffic flow*, Rend. Semin. Mat. Univ. Padova **131** (2014), 217–235, DOI 10.4171/RSMUP/131-13. MR3217759
- [8] E. Cristiani and S. Sahu, *On the micro-to-macro limit for first-order traffic flow models on networks*, Netw. Heterog. Media **11** (2016), no. 3, 395–413, DOI 10.3934/nhm.2016002. MR3541527
- [9] M. Di Francesco and M. D. Rosini, *Rigorous derivation of nonlinear scalar conservation laws from follow-the-leader type models via many particle limit*, Arch. Ration. Mech. Anal. **217** (2015), no. 3, 831–871, DOI 10.1007/s00205-015-0843-4. MR3356989
- [10] A. F. Filippov, *Differential equations with discontinuous righthand sides*, Mathematics and its Applications (Soviet Series), vol. 18, Kluwer Academic Publishers Group, Dordrecht, 1988. Translated from the Russian. MR1028776
- [11] T. Gimse and N. H. Risebro, *Riemann problems with a discontinuous flux function*, Third International Conference on Hyperbolic Problems, Vol. I, II (Uppsala, 1990), Studentlitteratur, Lund, 1991, pp. 488–502. MR1109304
- [12] G. Guerra and W. Shen, *Vanishing Viscosity Solutions of Riemann Problems for Models in Polymer Flooding*, Preprint (2016).
- [13] H. Holden and N. H. Risebro, *Continuum Limit Of Follow-The-Leader Models – a short proof*, To appear in DCDS (Preprint 2017).
- [14] ———, *Follow-the-Leader Models can be viewed as a numerical approximation to the Lighthill-Whitham-Richards model for traffic flow*, Preprint (2017).
- [15] S. N. Kružkov, *First order quasilinear equations with several independent variables.*, Mat. Sb. (N.S.) **81** (123) (1970), 228–255 (Russian). MR0267257
- [16] M. J. Lighthill and G. B. Whitham, *On kinematic waves. II. A theory of traffic flow on long crowded roads*, Proc. Roy. Soc. London. Ser. A. **229** (1955), 317–345, DOI 10.1098/rspa.1955.0089. MR0072606

- [17] E. Rossi, *A justification of a LWR model based on a follow the leader description*, Discrete Contin. Dyn. Syst. Ser. S **7** (2014), no. 3, 579–591, DOI 10.3934/dcdss.2014.7.579. MR3177735
- [18] W. Shen, *On the uniqueness of vanishing viscosity solutions for Riemann problems for polymer flooding*, NoDEA Nonlinear Differential Equations Appl. **24** (2017), no. 4, Art. 37, 25, DOI 10.1007/s00030-017-0461-y. MR3663611
- [19] \_\_\_\_\_, *Scilab codes for simulations and plots used in this paper*, Web: [www.personal.psu.edu/wxs27/SIM/Traffic-DDDE](http://www.personal.psu.edu/wxs27/SIM/Traffic-DDDE).
- [20] W. Shen and K. Shikh-Khalil, *Traveling Waves for a Microscopic Model of Traffic Flow*, Preprint 2017.